

FURTHER EXPERIMENTS ON IMPACT-PRESSURE  
PROBES IN A LOW-DENSITY,  
HYPERVELOCITY FLOW

By  
A. B. Bailey  
von Kármán Gas Dynamics Facility  
ARO, Inc.  
a subsidiary of Sverdrup and Parcel, Inc.

November 1962  
ARO Project No. 306159

# *Contrails*

**FOREWORD**

The author wishes to acknowledge the assistance of W. H. Sims in performing these experiments and the suggestions of J. L. Potter in analyzing the results.

# *Contrails*

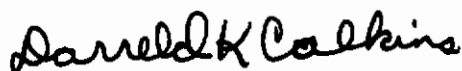
**ABSTRACT**

An experimental investigation of the behavior of flat-faced, impact-pressure probes with a range of orifice-to-probe diameter ratios was made in heated argon under conditions where  $M_\infty = 4$  to 14,  $T_0 = 2700$  to 4300°K, and  $Re_2/in. = 30$  to 430. At the lower Reynolds numbers the measured impact pressure was found to decrease with the pressure sensing orifice size. This result agrees with that found in heated nitrogen. As the Reynolds number increased this orifice effect became less significant, and at the higher Reynolds numbers no decrease in measured impact pressure was noted for the smallest orifice tested. This tends to confirm the assumption made in Ref. 1 that this behavior is caused by a thermomolecular flow effect. Because this effect is a function solely of pressure at a particular temperature, the greater the pressure the smaller the effect.

When  $Re_2 \sqrt{\rho_2/\rho_\infty}$  is less than 800 in argon the measured impact pressure was less than the true impact pressure and decreased to a minimum value, approximately 93 percent of the true value. As the Reynolds number decreased still further, the viscous effects became dominant, and there was a sharp increase in the measured impact pressure.

**PUBLICATION REVIEW**

This report has been reviewed and publication is approved.



Darreld K. Calkins  
Major, USAF  
AF Representative, VKF  
DCS/Test



Jean A. Jack  
Colonel, USAF  
DCS/Test

# *Contrails*

CONTENTS

	<u>Page</u>
ABSTRACT . . . . .	v
NOMENCLATURE . . . . .	ix
1.0 INTRODUCTION . . . . .	1
2.0 APPARATUS	
2.1 Wind Tunnel Description and Performance . . . . .	1
2.2 Tunnel Operating Conditions . . . . .	2
3.0 PROCEDURE . . . . .	3
4.0 DISCUSSION OF RESULTS	
4.1 Effect of Orifice Size on Impact Pressure . . . . .	3
4.2 Effect of Probe Diameter on the Measured Impact Pressure . . . . .	4
5.0 CONCLUSIONS . . . . .	6
REFERENCES . . . . .	7

TABLE

1. Flow Conditions . . . . .	9
------------------------------	---

ILLUSTRATIONS

Figure

1. Schematic Drawing of LDH Tunnel Nozzle, Tank, and Diffuser Area . . . . .	11
2. Variation of Measured Impact Pressure with Orifice-to-Probe Diameter Ratio . . . . .	12
3. Variation of Measured Impact Pressure with Reynolds Number and Density Ratio Behind a Normal Shock . . . . .	20
4. A Comparison of Impact-Pressure Measurements at Low Reynolds Numbers . . . . .	21

# *Contrails*



**NOMENCLATURE**

D	Outside diameter of the impact-pressure probe
$M_\infty$	Free-stream Mach number
$\dot{m}$	Mass flow rate
$p_{0c}$	Reservoir pressure (cold flow)
$p_{0h}$	Reservoir pressure (hot flow)
$p'_{0m}$	Measured impact pressure
$p'_{0i}$	Ideal impact pressure
$Re_\infty$	Reynolds number based on outside probe diameter and free-stream conditions
$Re_2$	Reynolds number based on outside probe diameter and conditions behind a normal shock
$T_{0c}$	Reservoir temperature of gas (cold flow)
$T_{0h}$	Reservoir temperature of gas (hot flow)
$T_w$	Wall temperature
$\lambda_2$	Mean free path based on conditions behind a normal shock
$\rho_\infty$	Density in free stream
$\rho_2$	Density behind the normal shock

# *Contrails*

## 1.0 INTRODUCTION

As far as is known to the author, the results presented in Ref. 1 for the behavior of impact-pressure probes in a low-density, hypervelocity flow represent the only available experimental data for such conditions in a diatomic gas. It was shown in that investigation that not only was there the expected viscous effect which modified the pressure measured by an impact probe but that there was also an effect associated with the size of the pressure sensing orifice. This report extends these earlier experiments by presenting results from tests under similar low-density, hypervelocity conditions in argon, a monatomic gas. In the present series of tests, argon was used as the working gas because it offered the opportunity to examine the behavior of the probes in a monatomic gas for which theory predicts a result different from that for a diatomic gas. Also, the characteristics of argon are such that a wide range of tunnel operating conditions could be established with relative simplicity compared to other gases.

## 2.0 APPARATUS

### 2.1 WIND TUNNEL DESCRIPTION AND PERFORMANCE

The Low-Density, Hypervelocity (LDH) Wind Tunnel is a continuous-flow, high-enthalpy wind tunnel in operation at the von Kármán Gas Dynamics Facility (VKF) of the Arnold Engineering Development Center (AEDC), Air Force Systems Command (AFSC), US Air Force. Briefly, the tunnel consists of a d-c arc heater, a stilling chamber, a conical nozzle of 30-deg total angle, a test chamber with instrumentation, a diffuser and a pumping system. A schematic drawing identifying some of the components is shown in Fig. 1. A complete description of the LDH tunnel is given in Ref. 2.

In the present tests a number of simple, water-cooled, brass, conical nozzles with a 30-deg total angle was used to accelerate the flow to supersonic speeds. The brass sections have throat diameters of 0.200, 0.397, and 0.750 inches, which produce Mach numbers at the exit plane in the range from 4 to 8.5. They can be used in conjunction with an aluminum

---

Manuscript released by author October 1962.

cone-frustum extension of 30-deg total angle which continues the expansion of the three basic nozzles to the Mach number range from 7 to 14.

When argon is the working gas the arc heater operates at less than 15 kw, the gas flow rate ranges from 1 to 30 lb/hr,  $T_{Oh}$  ranges from 2700 to 4300°K, and  $p_{Oh}$  ranges from 1.0 to 6.0 psia. At the nozzle exit and some distance downstream from it there is a clearly visible light blue jet surrounded in most cases by a pink region. On investigation with an impact-pressure probe the light blue region was found to correspond approximately to the high speed core of flow. The colors in the flow are thought to be caused by the excitation of a metastable argon state.

Good inflow characteristics to the nozzles under test were obtained by using a 3-in. -diam settling chamber upstream of the nozzle throat, having a length of 4 in. for the 0.200 and 0.397-in. -diam throats and 8 in. for the 0.750-in.-diam throat.

A complete description of the gas flow control, pressure measuring system, reservoir temperature estimate, test probes, and holder is given in Ref. 1. With regard to the reservoir temperature estimate, the fact that argon is monatomic considerably simplifies this estimate, since perfect gas laws apply. Hence, at constant mass flow, we have

$$T_{Oh} = T_{Oc} \left[ \frac{p_{Oh}}{p_{Oc}} \right]^2 \quad \dot{m} = \text{const}$$

## 2.2 TUNNEL OPERATING CONDITIONS

The useable flow regions existing in the conical nozzles were determined by making impact-pressure surveys. The most useable regions of flow usually corresponded to a condition where the nozzle flow was underexpanded and the nozzle shock was a considerable distance downstream of the nozzle exit (> 6 in.). For some of the flow conditions, the flow was overexpanded. In these cases the nozzle shock occurred nearer the nozzle exit plane, and the useable flow region was close to the nozzle exit. Whether the flow was underexpanded or overexpanded, in all the flow conditions investigated there was an axial Mach number gradient. As in the series of tests reported in Ref. 1 this is not considered to be a serious problem because only conditions at the probe face are important. The main precaution to be taken is to ensure that the probes are brought to the same axial position in the flow. The question then arises as to whether it is the front face of the probe or the probe shock which has to be brought to the same axial position. In the present series of tests the front face of the probe has been brought to the same axial station each

time because of the difficulty of matching shock positions for all the probe sizes. However, if it is assumed that shock positions should be matched, it is possible that the largest diameter probes indicated as much as two percent higher impact pressures because of their more forward shock positions. This effect would diminish as the probe diameter is decreased. Thus, the minimum of the curve representing the present data on Figs. 3 and 4 may be approximately one percent low in  $p_{0m}'/p_{0i}'$ .

The flow conditions at which the probes were tested are listed in Table 1. The maximum probe size tested at a particular flow condition was dictated by the extent of the useable test region. For all the conditions this region was between 0.5 and 1.2 inches in diameter.

### 3.0 PROCEDURE

The desired nozzle flow was established by adjusting the gas flow rate and arc-heater power input to bring the reservoir conditions to the operating level. When these conditions were achieved the probe under test was brought to a predetermined axial station on the nozzle centerline. A cathetometer was used to fix the position of the probe face, and care was taken to ensure that during any run any necessary corrections caused by probe expansion were made.

### 4.0 DISCUSSION OF RESULTS

The present investigation can be divided into two parts, one on the effect of orifice-to-probe diameter on the measured impact pressure at low pressures and the other on the effect of probe diameter on the measured impact pressure at all pressures.

#### 4.1 EFFECT OF ORIFICE SIZE ON IMPACT PRESSURE

In Fig. 2 the measured impact pressure for a range of probe diameters is plotted versus the orifice-to-probe diameter ratio. In Figs. 2a, b, and c at a reservoir temperature of 4260°K the impact pressures decrease as the orifice diameter decreases. This is consistent with the data reported in Ref. 1. It will be noted that the percentage reduction for the conditions occurring in Figs. 2b and c is less than that occurring



in Fig. 2a. The main difference in these conditions is in the level of impact pressure; for the higher pressure the orifice effect is less. If, as has been suggested in Ref. 1, the reduction in pressure with decrease in orifice size is related to a thermomolecular flow effect, then the orifice effect would be smaller with an increase of impact pressure, as observed. In Ref. 3 it has been shown that if tubes of varying diameter with the same temperature difference between their ends have the same low pressure applied to the hot end of the tube, then the smallest tube will sense the lowest pressure at its cold end. This may be what occurred with the impact probe. The pressure sensing orifice is exposed to the pressure and temperature existing behind the normal shock at its upstream face and the colder gas inside the probe at its downstream face. The temperature difference across the orifice possibly caused the above-mentioned thermomolecular effect. The main difficulty lies in the fact that at this time it seems impossible to assign any values to the gas temperature immediately upstream and downstream of the orifice. The problem is further complicated by the fact that the temperature behind the shock at very low Reynolds numbers becomes a function of the probe Reynolds number and temperature of the probe itself.

Levinsky and Yoshihara (Ref. 4) have shown an example wherein the maximum temperature behind the shock falls to 0.8 of the stagnation temperature as the Reynolds number of a cooled hemispherical body decreases from 13,652 to 152. This complicates any calculation to correct the measured impact pressure for thermomolecular flow effects since the temperature upstream of the orifice is a function of Reynolds number as well as Mach number and stagnation temperature. From Ref. 1 we found how difficult it is to find a single temperature difference across the orifice which would provide a reasonable correction for all the probe diameters possibly because of changing fluid property distributions in the merged, viscous shock layer as Reynolds number varied.

For the data presented in Figs. 2d to h where the pressures in general are higher and the reservoir temperatures are lower, the orifice effect does not exist for the smallest orifice tested. Accordingly, for the high pressure and relatively low temperature investigations reported in section 4.2, only probes having orifice-to-probe diameter ratios of approximately 0.7 were studied. An approximately one percent decrease in impact pressure is occasionally shown in Fig. 2 at the right extremities of certain curves as was shown in Ref. 1. This possibly deserves further investigation, but the pressure decrease is not a significant factor in the present discussion because of its small magnitude.

#### 4.2 EFFECT OF PROBE DIAMETER ON THE MEASURED IMPACT PRESSURE

The most important factor in the calibration of an impact probe is a knowledge of the true impact pressure. In some of the earliest work on

impact-pressure probes (Ref. 5) in the Reynolds number range from 2 to 12 a linear relationship was found to exist between the measured impact pressure and the reciprocal of the probe diameter. This experimental fact together with some theoretical work to further substantiate it seems to indicate that impact pressure obtained by extrapolating to  $1/D = 0$  was the true impact pressure. The shortcomings of this extrapolation became apparent when Sherman (Ref. 6) showed that data plotted in this manner were nonlinear at the higher Reynolds numbers. This made it difficult to define accurately the true impact pressure under the flow conditions that Sherman encountered. In fact, Matthews (Ref. 7) shows that for  $Re_\infty = 100$  to 6000 the measured impact pressure was less than the true impact pressure. In his investigation the low Reynolds numbers were obtained by testing small probes in a well-calibrated, high density, hypersonic wind tunnel. Because the theoretical considerations of Probstein and Kemp (Ref. 8) and Levinsky and Yoshihara (Ref. 4) support the decrease of impact pressure at relatively high Reynolds numbers shown by Matthews, it would seem desirable to make tests to free-stream Reynolds numbers of at least 6000 when operating at Mach numbers greater than 5.5. To minimize the influence of varying Mach number, the parameter  $Re_2 \sqrt{\rho_2/\rho_\infty}$  is used in the present report; Matthews'  $Re_\infty = 6000$  corresponds to  $Re_2 \sqrt{\rho_2/\rho_\infty} = 2200$ .

Considerable operational flexibility is necessary to achieve such a high Reynolds number in a small, very low density tunnel such as the AEDC LDH tunnel. At the present time, such a degree of flexibility is not available, but it was possible to achieve a probe Reynolds number of approximately 1600 based on free-stream conditions or  $Re_2 \sqrt{\rho_2/\rho_\infty} = 800$ . If it is assumed that Matthews' experimentally determined value of  $p'_{0m}/p'_{0i}$  is correct at  $Re_2 \sqrt{\rho_2/\rho_\infty} = 800$ , then the ratio  $p'_{0m}/p'_{0i}$  is 0.995. Thus, little error is likely in assuming that the impact pressure measured at the highest Reynolds numbers in the present experiments was the true or ideal value. Proof of this is shown when the data for  $M_\infty = 4.51$  and  $Re_2 \sqrt{\rho_2/\rho_\infty} = 801/in.$  are considered (Fig. 3). For the range of probe sizes investigated at this flow condition it was possible to define the  $p'_{0m}/p'_{0i}$  ratio over the range of  $Re_2 \sqrt{\rho_2/\rho_\infty}$  from 70 to 800. Using this curve, the true impact pressure for a probe at the next lower value of  $Re_2 \sqrt{\rho_2/\rho_\infty}$  was calculated, and the values of the ratio  $p'_{0m}/p'_{0i}$  were calculated for the range of probe sizes and plotted on the same figure. Using this bootstrap technique the variation of impact pressure was extended down to a value of  $Re_2 \sqrt{\rho_2/\rho_\infty} = 12.0$  For lower Reynolds

numbers than this a thermal-transpiration correction to the data is believed to be necessary, and no attempt will be made in this report to evaluate this.

Figure 3 shows that the minimum value of  $p'_{0m}/p'_{0i}$  is approximately 0.93 and that it is almost constant at this value over  $Re_2 \sqrt{\rho_2/\rho_\infty}$  range from 25 to 120. In Ref. 1 a comparison was made of some of the impact pressure probe data on the basis of free-stream Reynolds number. Apart from Matthews' results all the data shown in Ref. 1 indicate that for  $Re_\infty > 200$  the variation of  $p'_{0m}/p'_{0i}$  was constant and equal to unity. As a result of the present tests and those of Matthews it may be conjectured that the various low-density tunnel data may have shown an increase of a few percent in the ratio  $p'_{0m}/p'_{0i}$  if they had been extended to much higher Reynolds numbers.

The initial decrease of  $p'_{0m}/p'_{0i}$  with decreasing  $Re_2 \sqrt{\rho_2/\rho_\infty}$  is in agreement with that predicted by Levinsky and Yoshihara. Probstein and Kemp also predict this decrease, but their calculated decrease is greater than that predicted by Levinsky and Yoshihara. However, Probstein and Kemp also show that diatomic and monatomic gases behave differently, and the difference they predict is in qualitative agreement with the difference shown to exist between the present monatomic argon data and Matthews' diatomic air data. A comparison of these theoretical and experimental data is shown in Fig. 4.

The data of Matthews and the present investigation cannot be compared directly because in the former case  $T_w \approx T_o$ , whereas in this investigation  $T_w \approx 0.25T_o$ . However, in Ref. 4 it is stated that there is no significant difference between the theoretically calculated impact pressures obtained for both cold and adiabatic wall conditions. Therefore, it is probably not very misleading to assume that the heat-transfer effect is small, at least under conditions corresponding to the higher Reynolds numbers.

Also shown in Fig. 4 are some data on water-cooled, hemispherical-nosed, impact-pressure probes. The difference between these data and the flat-faced data may be attributable to the difference in shape and wall temperature.

## 5.0 CONCLUSIONS

It has been shown that as the pressure sensing orifice size decreased the measured impact pressure decreased at the lower Reynolds numbers in



the present series of tests in argon. This is in agreement with the results obtained for nitrogen in Ref. 1. Furthermore it is shown that, as the level of the impact pressure increased at a constant reservoir temperature, then there was less decrease in measured pressure with decrease in orifice size. In fact, at some of the highest impact pressures encountered, there was no decrease in measured pressure with decrease in orifice size. This seems to provide some qualitative support of the suggestion made in Ref. 1 that this measured pressure decrease was caused by a thermomolecular flow effect attributable to a temperature difference across the pressure sensing orifice.

Over the Reynolds number range where there was no thermomolecular flow effect, as the Reynolds number decreased, the ratio  $p_{o'm}^1/p_{o'i}^1$  decreased to a minimum of approximately 0.93 in argon and then, with further decrease in Reynolds number, the viscous effects became significant, and the ratio increased rapidly. According to this investigation the decrease of impact pressure at intermediate Reynolds numbers appears to be greater in argon than in air. This is predicted by the theoretical analysis of Ref. 8, although the theory overestimates the amount of the decrease. The theory of Ref. 4 yields results in closer agreement with our experiments but again seems to overestimate the decrease of impact pressure. Both theories fail to predict the upward trend of impact pressure that begins when very low Reynolds numbers are attained; the theoretical flow models are not applicable in that case. Thus, comparison with these theoretical results should be confined to the intermediate Reynolds numbers. Because of the complexity of the theoretical analysis of the problem, confirmation of these theories in a qualitative sense is a tribute to their originators. It also adds further proof to the often questioned possibility that  $p_{o'm}^1/p_{o'i}^1$  may fall below unity in the intermediate range of Reynolds numbers prior to its rapid increase at still lower Reynolds numbers.

#### REFERENCES

1. Bailey, A. B. and Boylan, D. E. "Some Experiments on Impact-Pressure Probes in a Low-Density Hypervelocity Flow." AEDC-TN-61-161, December 1961.
2. Potter, J. L., Kinslow, M., Arney, G. D., Jr., and Bailey, A. B. "Description and Preliminary Calibration of a Low-Density Hypervelocity Wind Tunnel." AEDC-TN-61-83, August 1961.
3. Arney, G. D., Jr., and Bailey, A. B. "Addendum to An Investigation of the Equilibrium Pressure Along Unequally Heated Tubes." AEDC-TDR-62-188, October 1962.

4. Levinsky, E. S. and Yoshihara, H. "Rarefied Hypersonic Flow Over a Sphere." Hypersonic Flow Research, Progress in Astronautics and Rocketry, Vol. 7, August 16-18, 1961, Academic Press, 1962, pp. 81-106.
5. Kane, E. D., and Schaaf, S. A. "Viscous Effects on Impact Probes in a Subsonic Rarefied Gas Flow." University of California Inst. of Eng. Research, Report No. HE-150-82, March 1951.
6. Sherman, F. S. "New Experiments on Impact Pressure Interpretation in Supersonic and Subsonic Rarefied Airstreams." University of California Inst. of Eng. Research, Report No. HE-150-99, December 1951.
7. Matthews, M. L. "An Experimental Investigation of Viscous Effects on Static and Impact Pressure Probes in Hypersonic Flow." Guggenheim Aeronautical Laboratory, California Inst. of Tech., Galcit-M-44, June 2, 1958.
8. Probst, Ronald F. and Kemp, Nelson H. "Viscous Aerodynamic Characteristics in Hypersonic Rarefied Gas Flow." Journal of the Aero/Space Sciences, Vol. 27, No. 3, March 1960, pp. 174-192.

TABLE 1  
FLOW CONDITIONS

m, lb/hr	P <sub>0c</sub> , psia	P <sub>0h</sub> , psia	Throat diam, in.	T <sub>0h</sub> , °K	M <sub>∞</sub>	Re <sub>2</sub> /in.	ρ <sub>2</sub> /ρ <sub>∞</sub>	Re <sub>2</sub> √(ρ <sub>2</sub> /ρ <sub>∞</sub> )/in.	Re <sub>∞</sub> /in.
30.4	0.66	2.05	0.75	2894	4.52	430	3.477	801	1574
"	"	"	"	"	5.62	258	3.641	491	1310
"	"	"	"	"	7.12	135	3.763	261	986
15.4	0.335	1.015	"	2780	4.22	274	3.413	507	939
"	"	"	"	"	5.34	152	3.607	289	716
"	"	"	"	"	6.37	95	3.712	183	603
19.34	1.26	3.96	0.397	2990	6.70	296	3.737	572	1970
15.4	0.99	3.00	"	2755	7.02	214	3.760	414	1540
10.94	0.72	2.28	"	3010	6.75	165	3.74	318	1090
4.3	0.30	1.125	"	4260	5.22	109	3.592	208	480
4.3	0.30	1.125	"	4260	8.18	32.2	3.815	63	271
6.5	1.95	6.42	0.20	3280	9.18	178	3.849	350	2020
3.43	1.02	3.84	"	4260	8.55	97.3	3.829	190	897
6.5	1.95	6.42	"	3280	13.66	56.6	3.922	112	1284

# *Contrails*

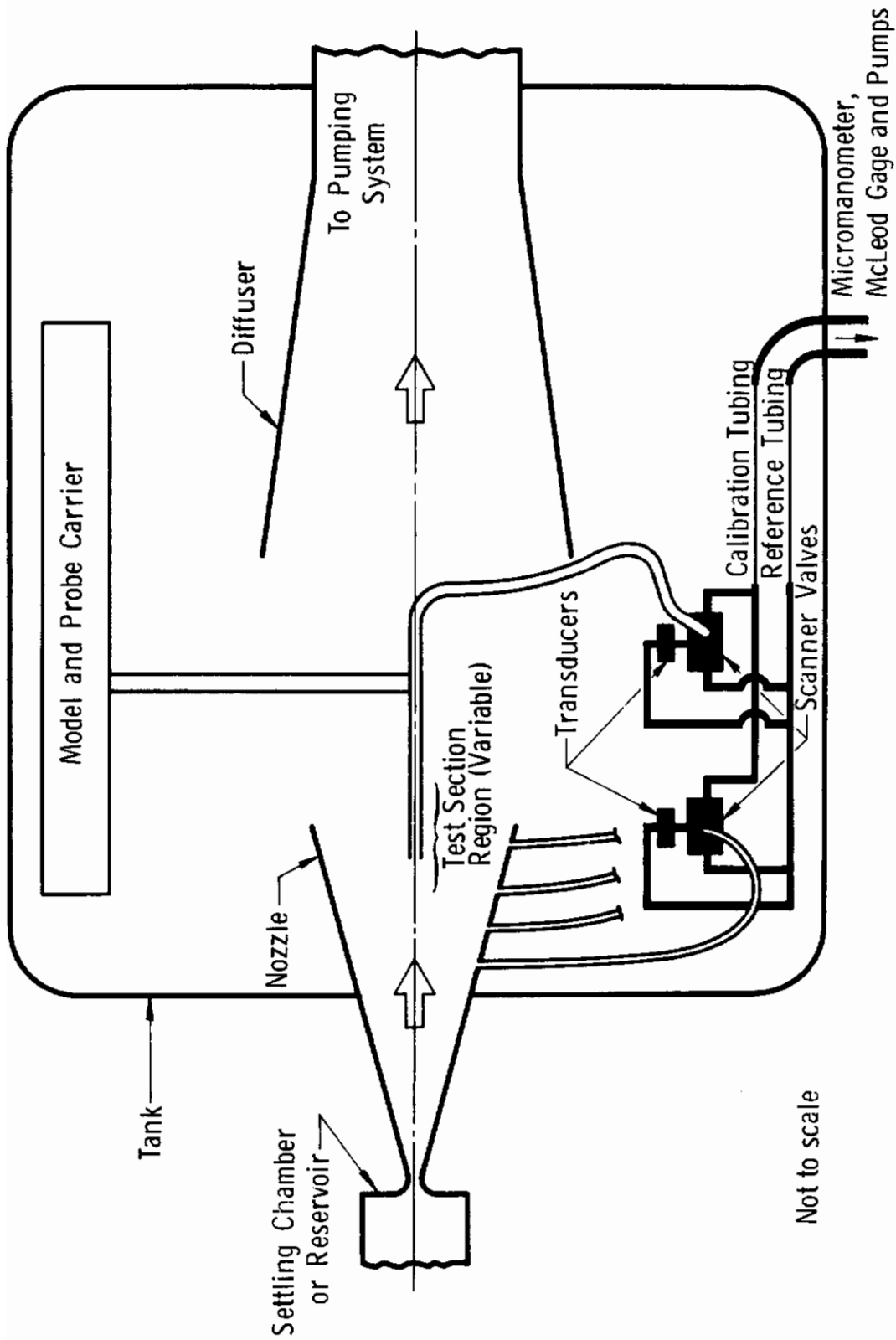


Fig. 1 Schematic Drawing of LDH Tunnel Nozzle, Tank, and Diffuser Area

## Argon

Throat Diameter = 0.397 in.

$\dot{m} = 4.3 \text{ lb/hr}$        $T_{o_h} = 4260^\circ\text{K}$

$p_{o_c} = 0.30 \text{ psia}$        $p_{o_h} = 1.125 \text{ psia}$

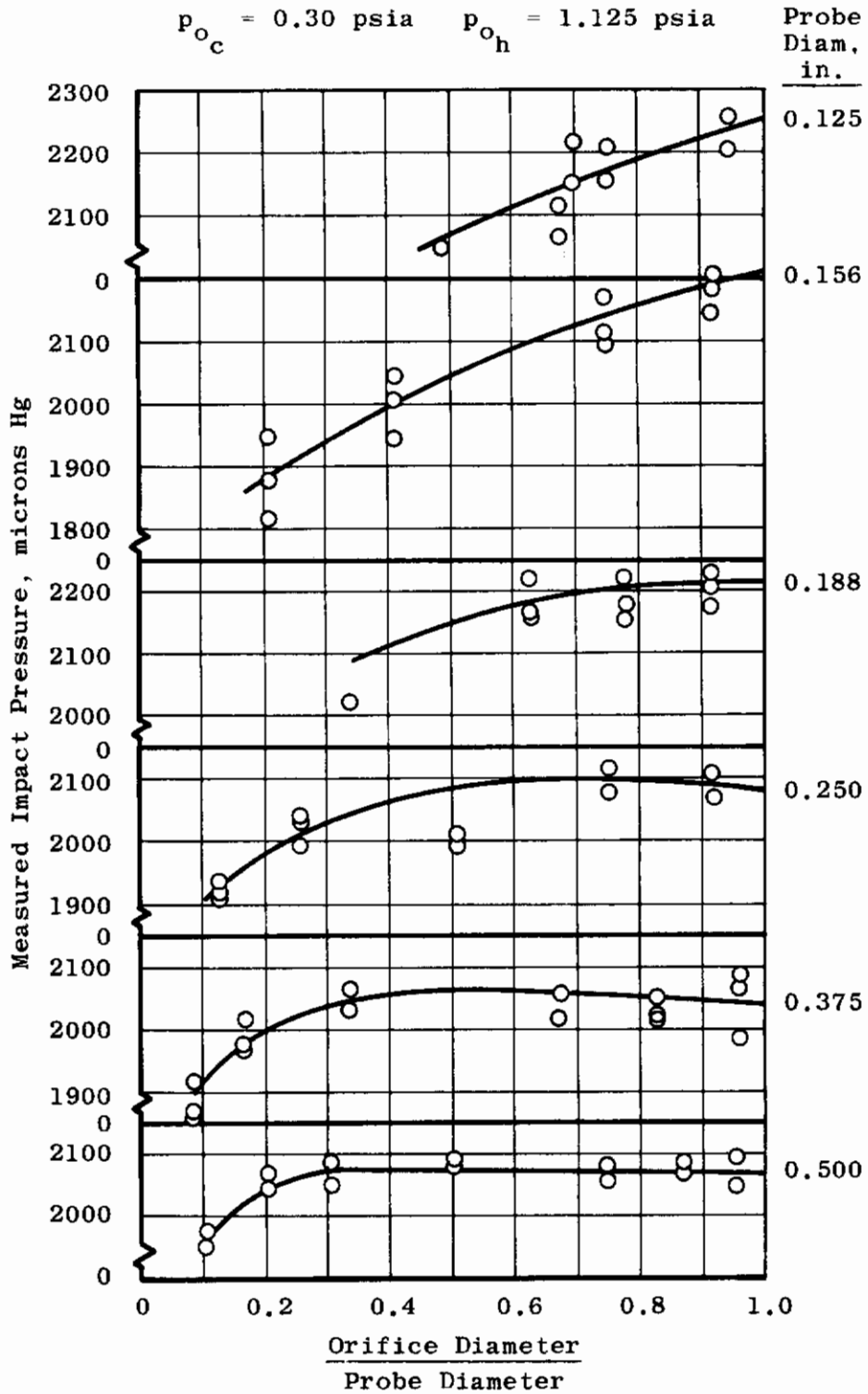


Fig. 2a Variation of Measured Impact Pressure with Orifice-to-Probe Diameter Ratio

Argon

Throat Diameter = 0.2 in.

$\dot{m} = 3.43 \text{ lb/hr}$        $T_{O_h} = 4260^\circ\text{K}$

$p_{O_c} = 1.02 \text{ psia}$        $p_{O_h} = 3.84 \text{ psia}$

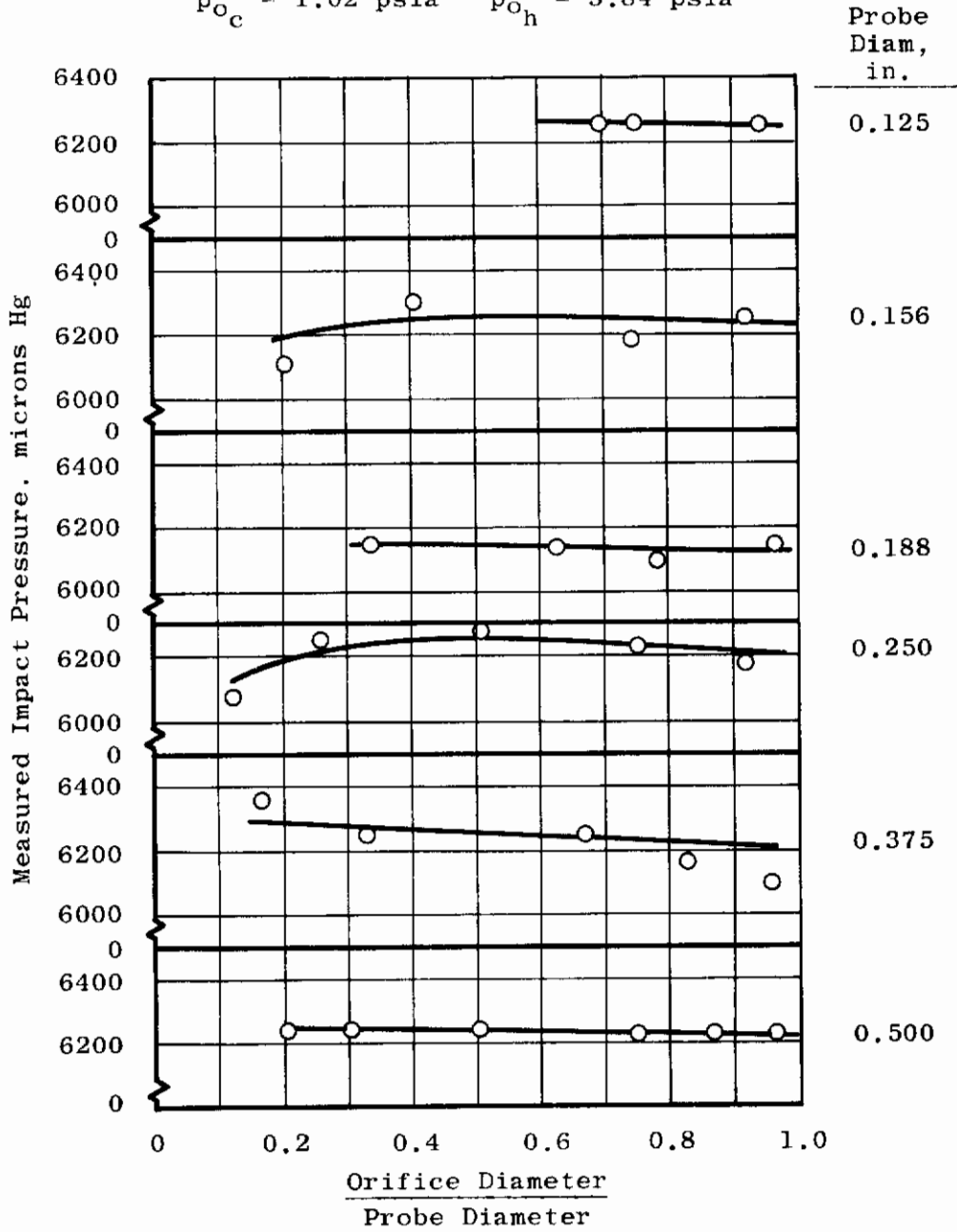


Fig. 2b Continued

## Argon

Throat Diameter = 0.397 in.

$\dot{m} = 4.3 \text{ lb/hr}$        $T_o = 4260^\circ\text{K}$

$p_{o_c} = 0.30 \text{ psia}$        $p_{o_h} = 1.125 \text{ psia}$

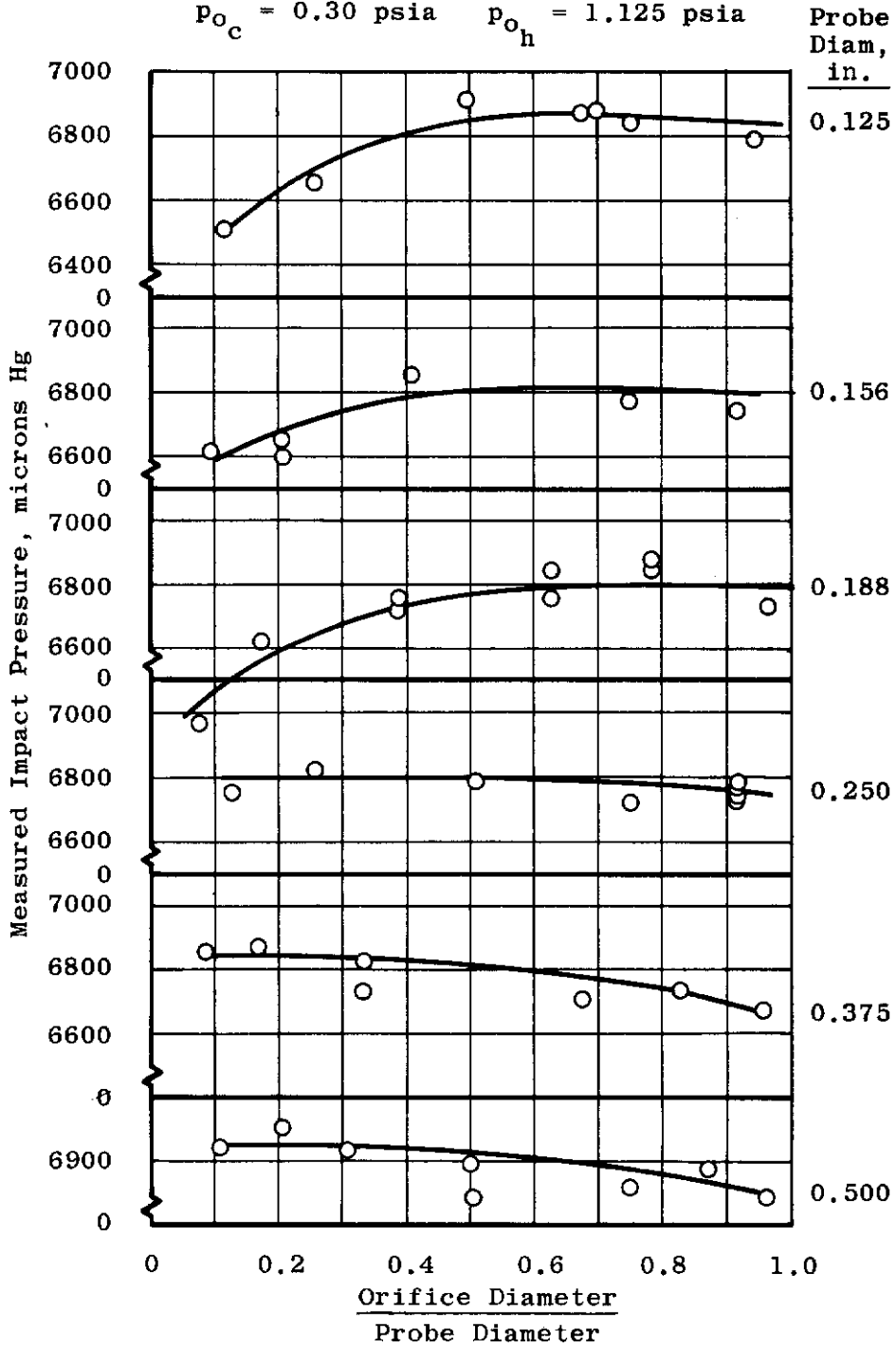


Fig. 2c Continued



Argon

Throat Diameter = 0.2 in.

$\dot{m} = 6.5$  lb/hr  $T_{O_h} = 3280^\circ\text{K}$

$p_{O_c} = 1.95$  psia  $p_{O_h} = 6.42$  psia

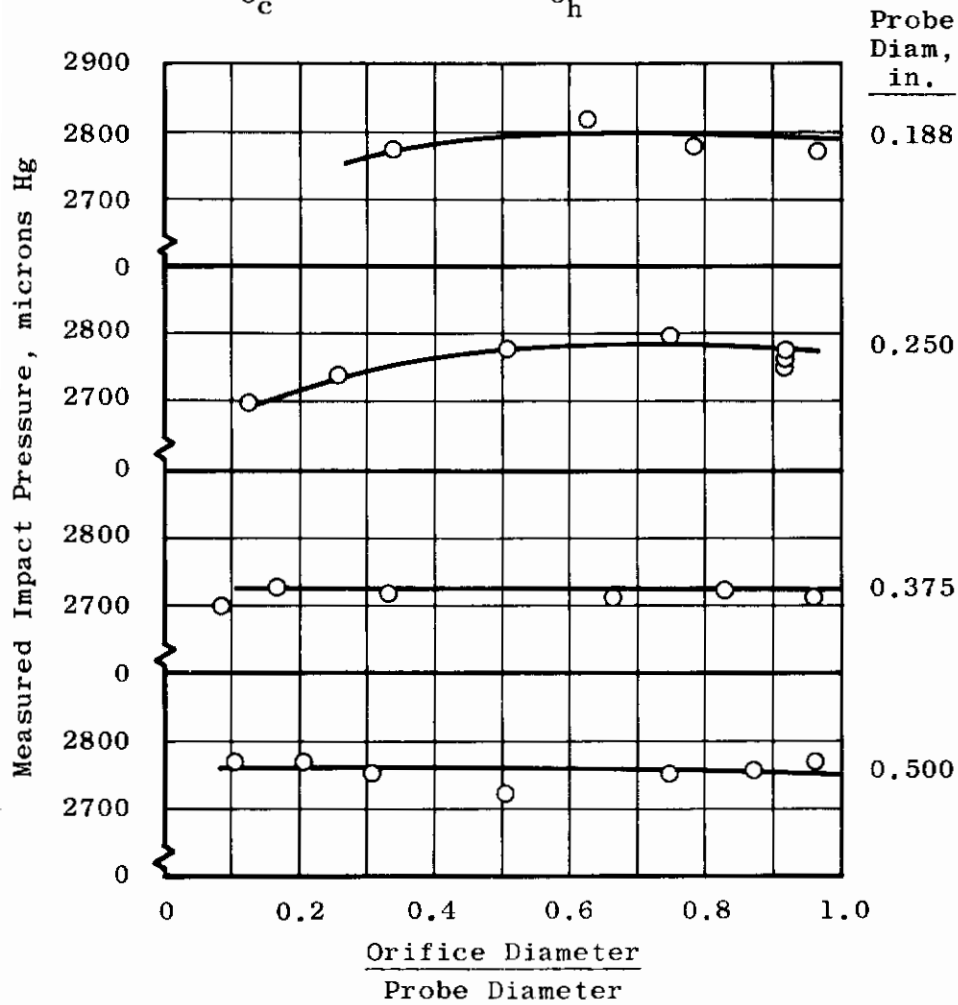


Fig. 2d Continued

Argon

Throat Diameter = 0.397 in.

$\dot{m} = 10.94$  lb/hr  $T_{O_h} = 3010^{\circ}\text{K}$

$p_{O_c} = 0.72$  psia  $p_{O_h} = 2.26$  psia

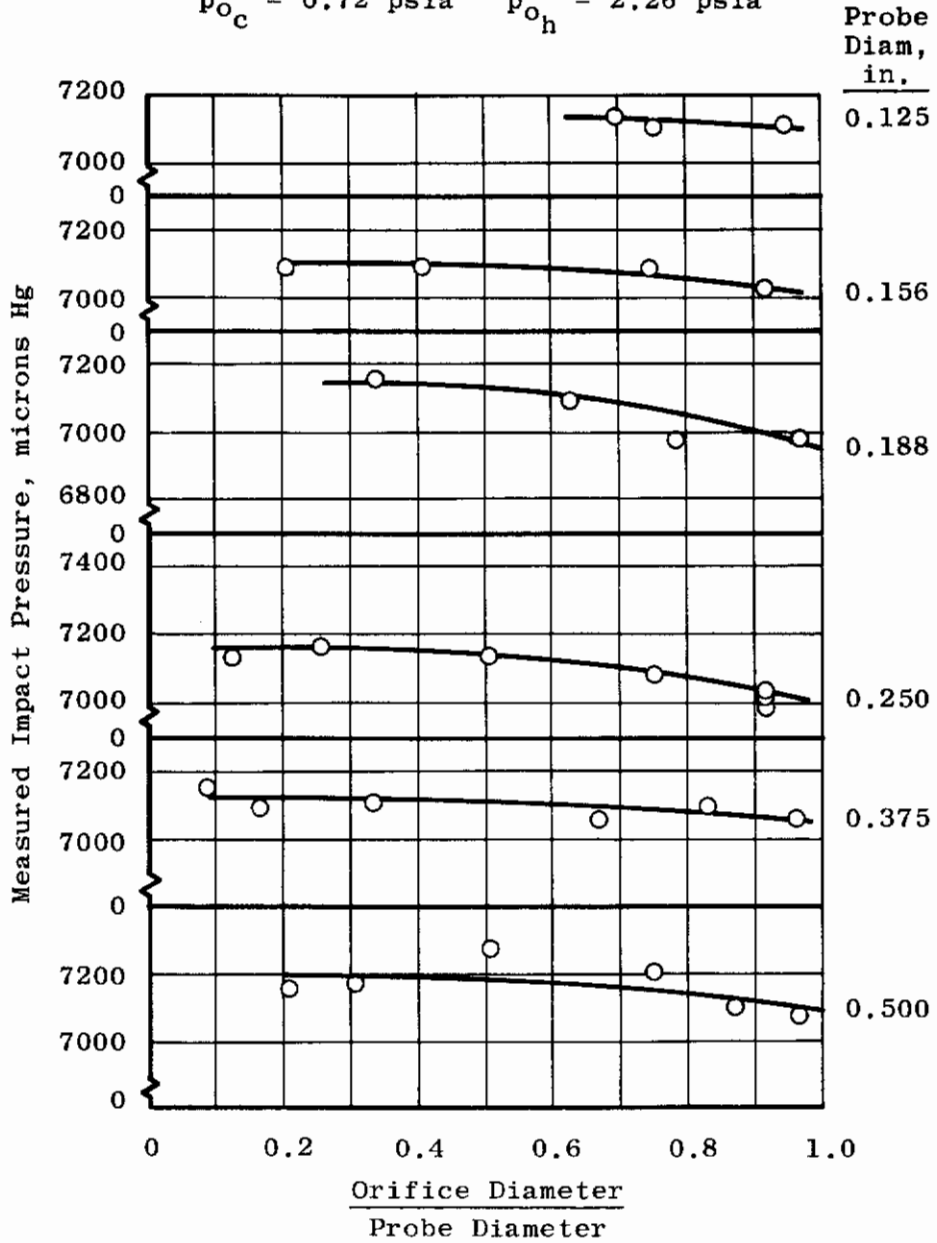


Fig. 2e Continued

Argon

Throat Diameter = 0.2 in.

$\dot{m} = 6.5 \text{ lb/hr}$        $T_{O_h} = 3280^\circ\text{K}$

$p_{O_c} = 1.95 \text{ psia}$        $p_{O_h} = 6.42 \text{ psia}$

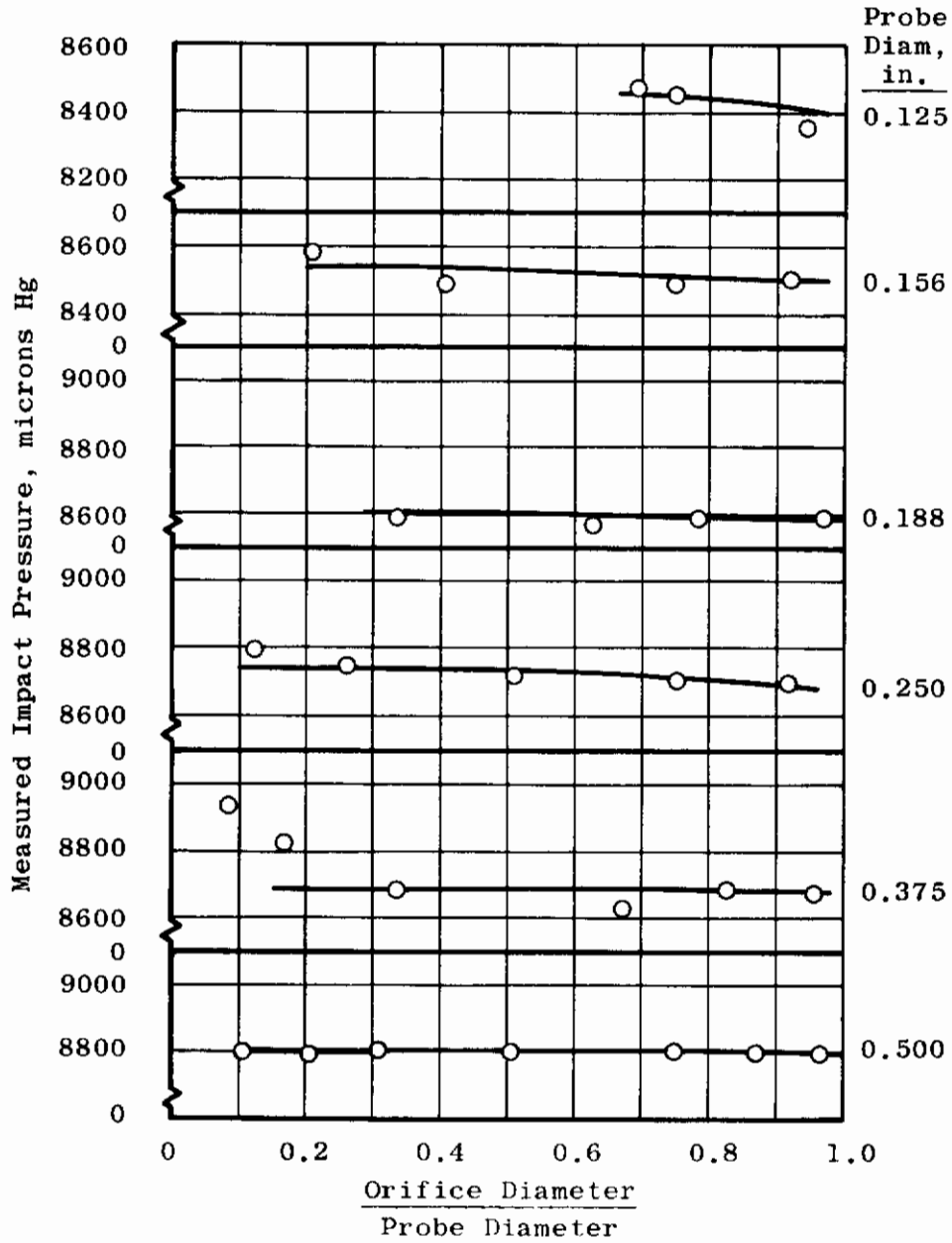


Fig. 2f Continued

Argon

Throat Diameter = 0.397 in.

$\dot{m} = 15.4$  lb/hr  $T_{o_h} = 2755^\circ\text{K}$

$p_{o_c} = 0.99$  psia  $p_{o_h} = 3.00$  psia

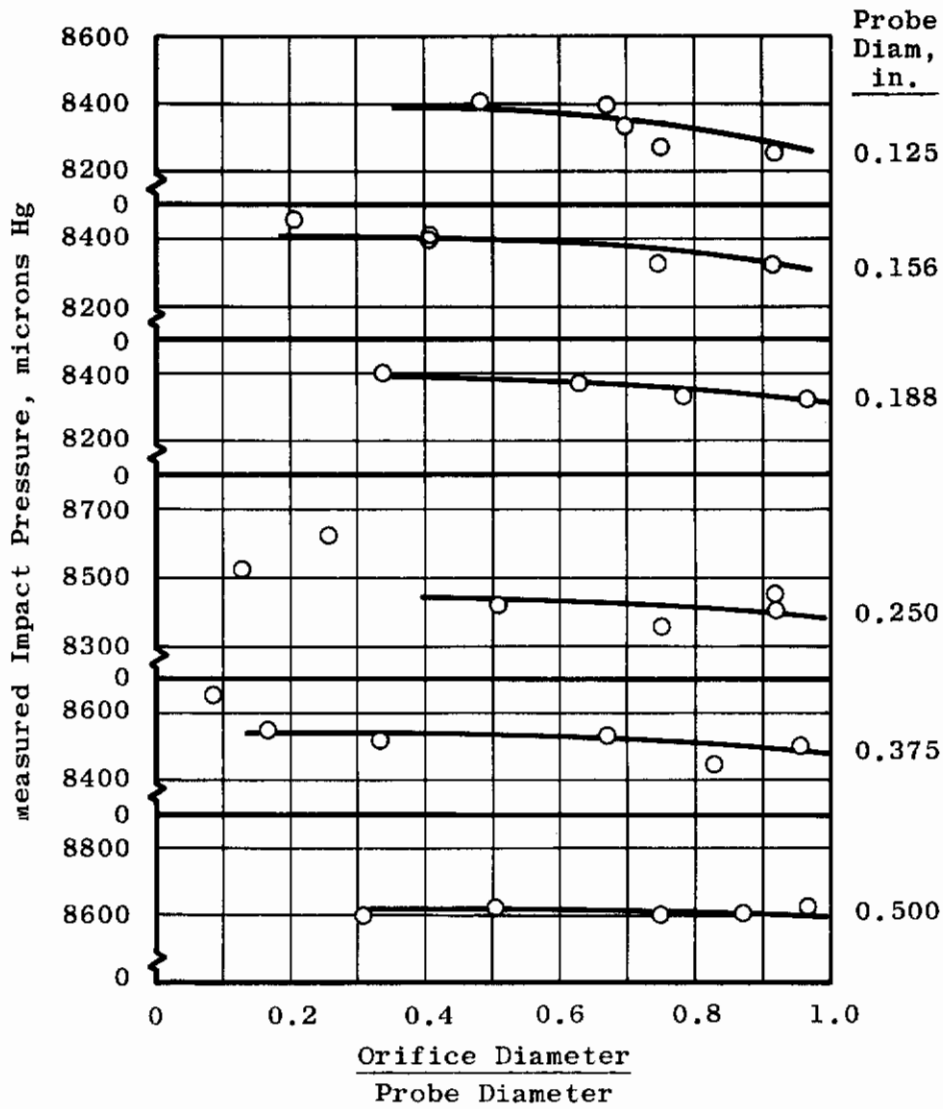


Fig. 2g Continued

### Argon

Throat Diameter = 0.397 in.

$\dot{m} = 19.34$  lb/hr      $T_{o_h} = 2990^\circ\text{K}$

$p_{o_c} = 1.26$  psia      $p_{o_h} = 3.96$  psia

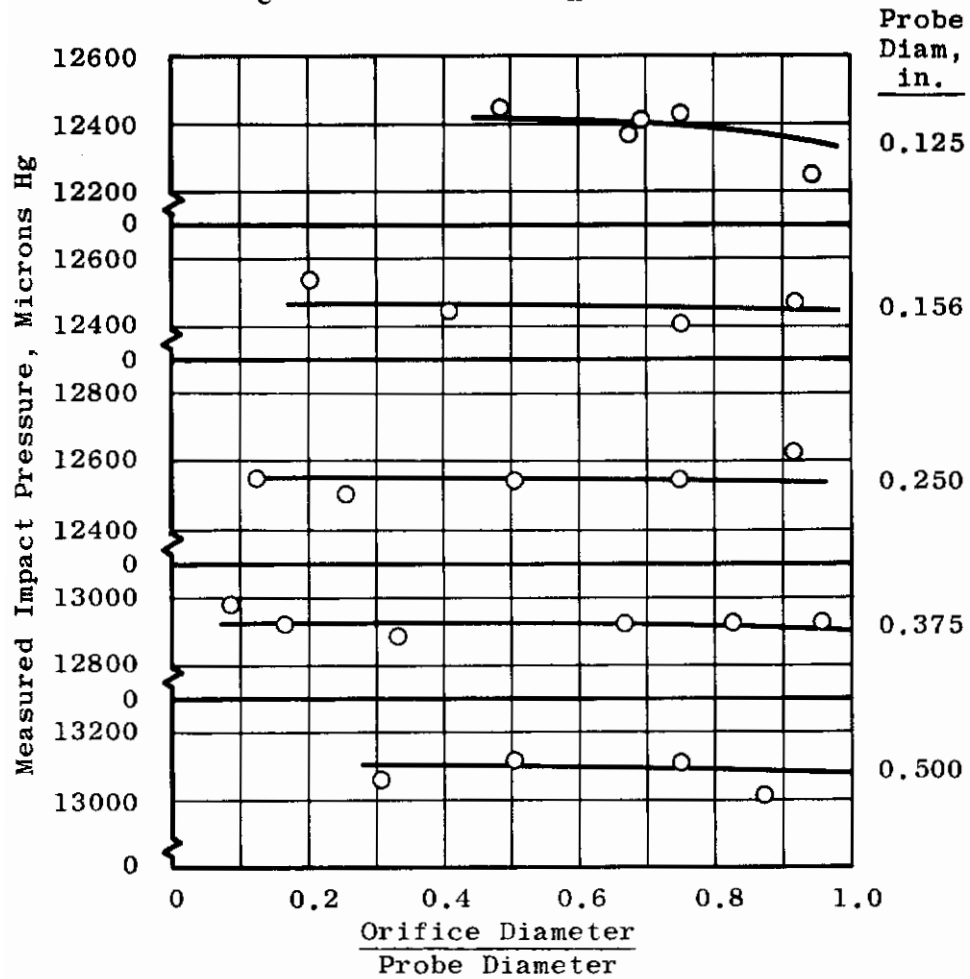


Fig. 2h Concluded

Flat-Faced Probes

Symbol	$M_{\infty}$	$T_{O_h}, ^\circ K$	$Re_2$	$\frac{P_2}{P_{\infty}}$ / in.
○	4.52	2894	801	In Argon
□	5.62	2894	491	
◇	7.02	2755	414	
▽	9.18	3280	350	
○	7.12	2894	261	
◇	4.22	2780	507	
☆	5.34	2780	289	
◇	6.37	2780	183	
△	6.70	2990	572	
●	6.75	3010	318	
■	5.22	4260	208	
◆	8.55	4260	190	
▲	13.66	3280	112	
▼	8.18	4260	63	

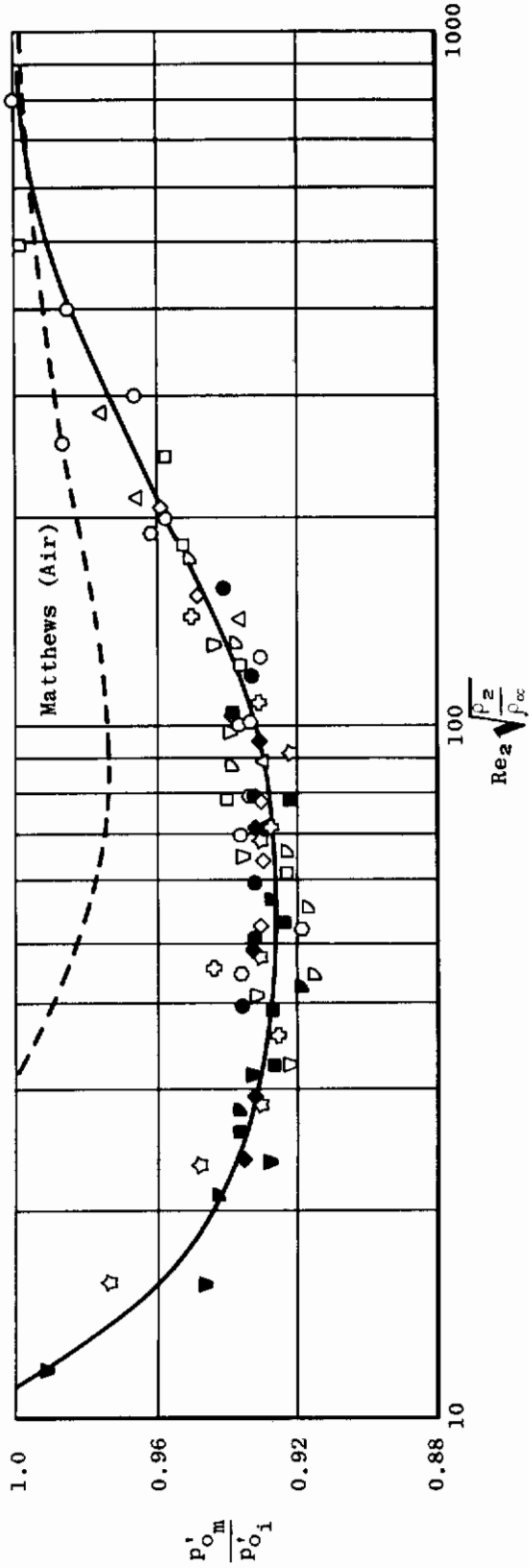


Fig. 3 Variation of Measured Impact Pressure with Reynolds Number and Density Ratio Behind a Normal Shock

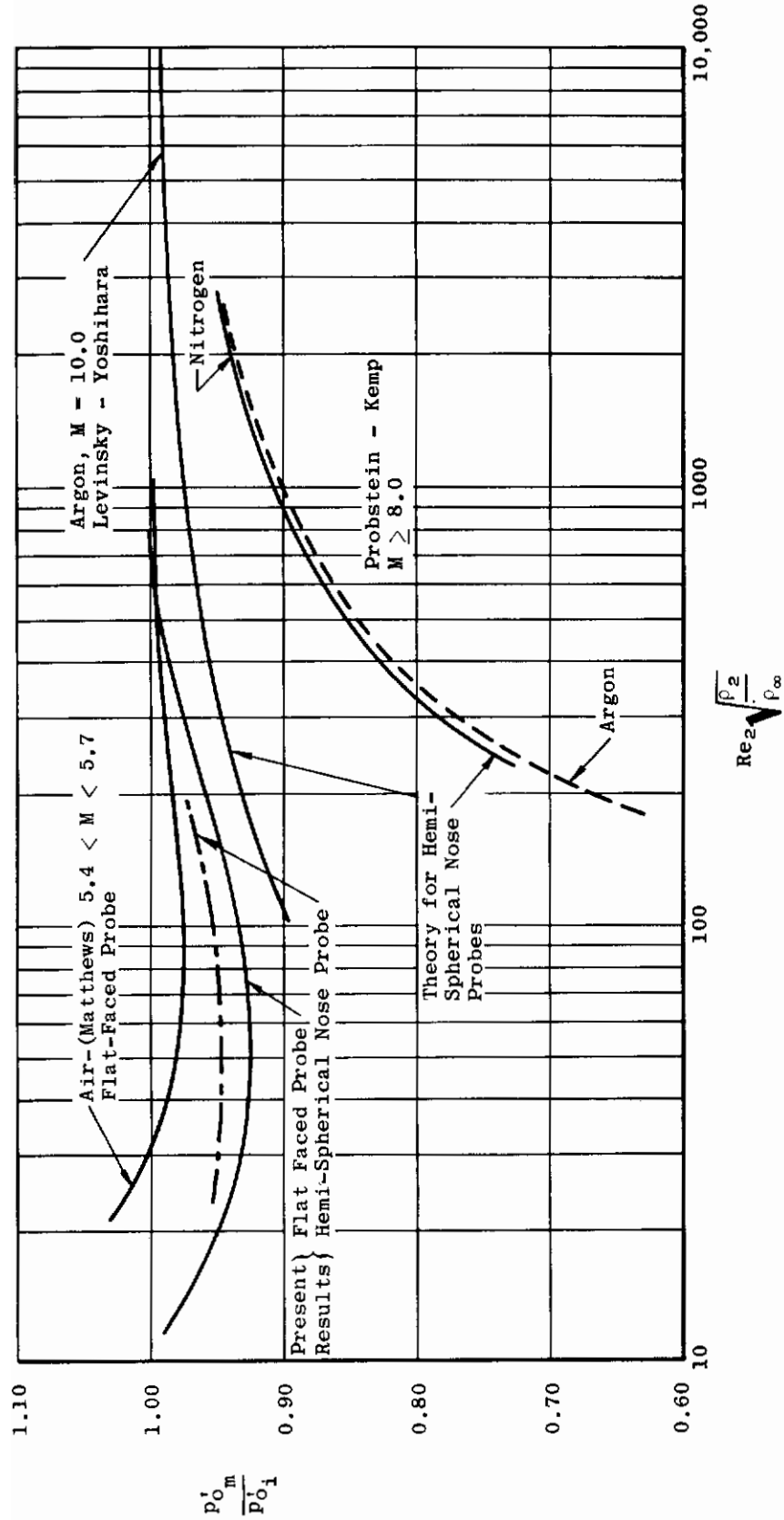


Fig. 4 A Comparison of Impact-Pressure Measurements at Low Reynolds Numbers

# *Contrails*